



Cite this: *New J. Chem.*, 2015,
39, 6117

1,4-Benzenedisulfonic acid (H_2BDS) as terephthalic acid analogue for the preparation of coordination polymers: the examples of $M(BDS)(NMP)_3$ ($M = Mn, Fe, Co$; $NMP = N$ -methylpyrrolidone)†

Christina Zitzer, Thomas W. T. Muesmann, Jens Christoffers* and Mathias S. Wickleder*

The solvothermal reactions of 1,4-benzenedisulfonic acid, H_2BDS , with suitable salts of manganese, iron, and cobalt led to the new disulfonates $M(BDS)(NMP)_3$ ($M = Mn, Fe, Co$), when *N*-methylpyrrolidone (NMP) was used as the solvent. The isotropic compounds crystallize with triclinic symmetry ($P\bar{1}$, $Z = 2$; $M = Mn$: $a = 916.84(3)$ pm, $b = 965.57(3)$ pm, $c = 1437.87(5)$ pm, $\alpha = 95.297(2)^\circ$, $\beta = 97.834(2)^\circ$, $\gamma = 92.576(2)^\circ$, $R_1/wR_2(I_0 > 2\sigma(I_0)) = 0.0300/0.0701$; $M = Fe$: $a = 911.98(5)$ pm, $b = 960.75(5)$ pm, $c = 1432.41(8)$ pm, $\alpha = 94.951(2)^\circ$, $\beta = 98.050(3)^\circ$, $\gamma = 92.029(2)^\circ$, $R_1/wR_2(I_0 > 2\sigma(I_0)) = 0.0238/0.0689$; $M = Co$: $a = 911.3(1)$ pm, $b = 959.5(1)$ pm, $c = 1428.6(2)$ pm, $\alpha = 94.791(5)^\circ$, $\beta = 98.229(5)^\circ$, $\gamma = 91.873(6)^\circ$, $R_1/wR_2(I_0 > 2\sigma(I_0)) = 0.0264/0.0684$). In the crystal structure, the M^{2+} ions (Mn^{2+} , Fe^{2+} and Co^{2+}) are in octahedral oxygen coordination of three monodentate disulfonate groups and three NMP molecules. The disulfonate groups link the metal ions into infinite layers. Thermoanalytical investigations showed that the desolvation of the compounds occurred in a temperature range between 50 °C and 330 °C. The solvent free sulfonates showed remarkable high stabilities up to nearly 500 °C. The thermal behaviour was investigated by DSC/TG measurements and X-ray powder diffraction.

Received (in Victoria, Australia)
26th January 2015,
Accepted 26th May 2015

DOI: 10.1039/c5nj00223k

www.rsc.org/njc

Introduction

Compounds that are composed of metallic nodes and organic linkers were synthesized in a great variety throughout the years. Depending on the dimensionality of the linkage and the porosity of the compounds, they are referred to as coordination polymers (CPs) and metal organic frameworks (MOFs). The interest in coordination polymers and MOFs has increased in recent times because such compounds may have interesting chemical and physical properties.¹ To date, CPs and MOFs are mostly constructed using carboxylates as linkers, because the related polycarboxylic acids are commercially available and cheap. Even if this is certainly advantageous, carboxylates do have significant disadvantages. One is the restricted thermal stability, due to easy decarboxylation upon heating. For example, copper(II) terephthalate decomposes already between 160 °C and 230 °C,² which is a severe problem if applications like gas storage are envisaged that usually cause the significant heating of the host lattice due to physi- and chemi-sorption. In contrast,

the sulfo analog copper(II)-1,4-benzenedisulfonate decomposes only at the remarkably high temperature of 400 °C.³ However, despite such outstanding properties, polysulfonates have not been investigated to a significant extent up to now. This has to do with the limited availability of the respective polysulfonic acids, which are commercially available only for a few examples.^{3–7} Even reliable syntheses protocols for these acids are lacking. In a systematic approach, we develop suitable synthetic routes for polysulfonic acids and to characterize the structural chemistry and the properties of polysulfonates. In the course of these investigations, we reported a large number of polysulfonic acids and polysulfonate based coordination polymers.^{3,8–10} Most of these compounds have been obtained for metals such as copper, zinc, and selected rare earth elements. Recently, we started to investigate other transition metals, and we reported some manganese polysulfonates based on 1,2,4,5-benzenetetrasulfonic acid and 1,4-benzenedisulfonic acid.¹¹ The latter is the sulfo analogue of terephthalic acid, which is frequently used for the synthesis of carboxylate based coordination polymers.¹² In this study, we present new coordination polymers based on 1,4-benzenedisulfonic acid (H_2BDS), namely, the transition metal compounds $M(BDS)(NMP)_3$ ($M = Mn, Fe, Co$), which were obtained in solvothermal reactions in *N*-methylpyrrolidone (NMP).

Institut für Chemie, Carl von Ossietzky-Universität Oldenburg, D-26111 Oldenburg, Germany. E-mail: mathias.wickleder@uni-oldenburg.de; Fax: +49 441/798 3873

† CCDC 967021, 967023 and 967024. For crystallographic data in CIF or other electronic format see DOI: 10.1039/c5nj00223k



Experimental section

Materials and instrumentation

$\text{Mn}(\text{CH}_3\text{COO})_3 \cdot 2\text{H}_2\text{O}$, $\text{FeCl}_2 \cdot 4\text{H}_2\text{O}$, $\text{Co}(\text{CH}_3\text{COO})_2$ and *N*-methylpyrrolidone were purchased from commercial sources and used as received. 1,4-Benzenedisulfonic acid was synthesized as reported previously.¹⁰

IR spectra were obtained on a Bruker Tensor 27 spectrometer equipped with a “GoldenGate” diamond-ATR unit. DSC/TG measurements were performed with the help of a thermal analyzer (TGA/DSC 1 STAR^e System, METTLER-TOLEDO). For that purpose, about 5 mg of each substance were filled into a corundum crucible and heated with a constant rate of 10 K min⁻¹. The thermal decompositions were monitored from 25 °C to 1050 °C in a flow of dry oxygen. The measurements were carried out under oxygen flow in order to avoid carbon forming at the end of the decomposition, which would falsify the calculated values of the degradation products. Characteristic points, like onset and end temperatures, of the thermal effects were taken from the DSC curve following common procedures using the software delivered with the analyser (Mettler-Toledo STARe V9.3).¹³

Syntheses

Manganese(II)(1,4-benzenedisulfonate)tris(*N*-methylpyrrolidone)

Mn(BDS)(NMP)₃. A mixture of 25 mg of $\text{Mn}(\text{CH}_3\text{COO})_3 \cdot 2\text{H}_2\text{O}$ (0.093 mmol), 20 mg of $\text{H}_2\text{BDS} \cdot 2\text{H}_2\text{O}$ (0.073 mmol), and 3 ml of NMP was filled into a glass ampoule. The ampoule was

torch-sealed under vacuum, placed in a resistance furnace and heated up to 110 °C for 6 h. After 36 h, the furnace was slowly cooled to room temperature for 200 h. In the organic solvent, Mn(III)-acetate disproportionates to Mn^{4+} (MnO_2) and Mn^{2+} . Furthermore, Mn^{2+} reacts with H_2BDS . The product was obtained as transparent colorless single crystals, which were separated from the supernatant by decantation.

IR(ATR): 2962 (w), 2880 (w), 1669 (m), 1647 (s), 1520 (m), 1483 (m), 1450 (m), 1430 (m), 1417 (m), 1401 (m), 1306 (m), 1237 (s), 1187 (s), 1137 (s), 1129 (s), 1106 (m), 1076 (m), 1047 (s), 1009 (s), 934 (m), 850 (m), 833 (m), 723 (m), 663 (s), 578 (s), 563 (s), 553 (m), 523 (m) cm⁻¹.

Iron(II)(1,4-benzenedisulfonate)tris(*N*-methylpyrrolidone) Fe(BDS)(NMP)₃. A mixture of 19 mg of $\text{FeCl}_2 \cdot 4\text{H}_2\text{O}$ (0.096 mmol), 20 mg of $\text{H}_2\text{BDS} \cdot 2\text{H}_2\text{O}$ (0.073 mmol) and 3 ml of NMP was filled into a glass ampoule. The torch-sealed ampoule was placed in a resistance furnace and heated up to 120 °C for 6 h. After 36 h, the furnace was slowly cooled to room temperature within 120 h. The product was obtained as transparent colorless single crystals, which were separated from the supernatant by decantation.

IR(ATR): 2970 (w), 2938 (w), 2883 (w), 1643 (s), 1517 (m), 1483 (w), 1449 (w), 1426 (w), 1410 (m), 1392 (w), 1307 (m), 1258 (w), 1213 (s), 1174 (s), 1105 (m), 1036 (s), 1001 (s), 835 (m), 660 (s), 617 (m), 578 (s), 546 (s) cm⁻¹.

Cobalt(II)(1,4-benzenedisulfonate)tris(*N*-methylpyrrolidone)

Co(BDS)(NMP)₃. A mixture of 39 mg of $\text{Co}(\text{CH}_3\text{COO})_2$ (0.220 mmol), 20 mg of $\text{H}_2\text{BDS} \cdot 2\text{H}_2\text{O}$ (0.073 mmol) and 3 ml of NMP was filled

Table 1 Crystallographic data of M(BDS)(NMP)₃ (M = Mn, Fe, Co)

	Mn(BDS)(NMP) ₃	Fe(BDS)(NMP) ₃	Co(BDS)(NMP) ₃
Chemical formula	$\text{C}_{21}\text{H}_{31}\text{N}_3\text{O}_9\text{S}_2\text{Mn}$	$\text{C}_{21}\text{H}_{31}\text{N}_3\text{O}_9\text{S}_2\text{Fe}$	$\text{C}_{21}\text{H}_{31}\text{N}_3\text{O}_9\text{S}_2\text{Co}$
Chemical formula weight	588.55 g mol ⁻¹	589.46 g mol ⁻¹	592.54 g mol ⁻¹
Lattice parameters	$a = 916.84(3)$ pm $b = 965.57(3)$ pm $c = 1437.87(5)$ pm $\alpha = 95.297(2)^\circ$ $\beta = 97.834(2)^\circ$ $\gamma = 92.576(2)^\circ$	$a = 911.98(5)$ pm $b = 960.75(5)$ pm $c = 1432.41(8)$ pm $\alpha = 94.951(2)^\circ$ $\beta = 98.050(3)^\circ$ $\gamma = 92.029(2)^\circ$	$a = 911.3(1)$ pm $b = 959.5(1)$ pm $c = 1428.6(2)$ pm $\alpha = 94.791(5)^\circ$ $\beta = 98.229(5)^\circ$ $\gamma = 91.873(6)^\circ$
Density (calculated) (g cm ⁻³)	1.56	1.58	1.60
Cell volume (Å ³)	1253.51(7)	1236.6(1)	1230.7(3)
No. of formula units	2	2	2
Cryst syst.	Triclinic	Triclinic	Triclinic
Space group	$P\bar{1}$ (no. 2)	$P\bar{1}$ (no. 2)	$P\bar{1}$ (no. 2)
Measuring device	Bruker APEX II	Bruker APEX II	Bruker APEX II
Radiation	Mo-K α (graphite monochromatized, $\lambda = 71.07$ pm)	Mo-K α (graphite monochromatized, $\lambda = 71.07$ pm)	Mo-K α (graphite monochromatized, $\lambda = 71.07$ pm)
Temperature (K)	120	120	120
Index range	$-15 \leq h \leq 15$ $-16 \leq k \leq 16$ $-23 \leq l \leq 23$	$-16 \leq h \leq 16$ $-17 \leq k \leq 17$ $-26 \leq l \leq 26$	$-16 \leq h \leq 16$ $-17 \leq k \leq 17$ $-20 \leq l \leq 25$
Absorption correction	Numerical	Numerical	Empirical
μ (cm ⁻¹)	7.49	8.36	9.24
Measured reflections	67 956	90 529	63 891
Unique reflections	12 143	13 013	12 950
With $I_0 > 2\sigma(I_0)$	8927	11 455	11 020
R_{int} ; R_σ	0.0425; 0.0445	0.0306; 0.0179	0.0301; 0.0245
Structure determination	SHELXS97 and SHELXL97	SHELXS97 and SHELXL97	SHELXS97 and SHELXL97
Scattering factors	Intern. tables, vol. C	Intern. tables, vol. C	Intern. tables, vol. C
GOF	0.936	1.069	1.024
R_1 ; $wR_2(I_0 > 2\sigma(I_0))$	0.0300; 0.0701	0.0238; 0.0689	0.0264; 0.0684
R_1 ; wR_2 (all data)	0.0482; 0.0745	0.0278; 0.0705	0.0344; 0.0720
Max./min. electron density	1.095/−0.743 e Å ⁻³	1.661/−0.737 e Å ⁻³	1.032/−0.430 e Å ⁻³
CCDC	967024	967021	967023



Table 2 Selected distances (pm) and angles (deg) for the disulfonates $M(BDS)(NMP)_3$ ($M = Mn, Fe, Co$)

	M	Mn	Fe	Co
[MO_6]	M-O1	220.78(7)	216.49(5)	212.75(6)
	M-O2	212.57(7)	206.13(5)	204.53(6)
	M-O3	216.56(7)	209.27(5)	207.90(6)
	M-O11	216.45(7)	213.96(5)	210.13(6)
	M-O12	218.83(7)	214.65(5)	210.23(6)
	M-O14	216.53(7)	213.07(5)	209.44(6)
	O1-M-O2	90.79(3)	89.66(2)	89.95(2)
	O1-M-O3	94.87(3)	95.37(2)	94.27(2)
	O1-M-O11	175.70(3)	175.36(2)	176.05(2)
	O1-M-O12	84.72(3)	85.59(2)	86.42(2)
	O1-M-O14	89.83(3)	90.68(2)	90.36(2)
	O2-M-O3	173.39(3)	173.60(2)	173.87(2)
	O2-M-O11	85.08(3)	85.71(2)	86.09(2)
	O2-M-O12	90.52(3)	89.26(2)	89.85(3)
	O2-M-O14	92.80(3)	93.58(2)	92.88(3)
[SO_3]	O3-M-O11	89.32(3)	89.27(2)	89.67(2)
	O3-M-O12	86.61(3)	87.19(2)	85.99(3)
	O3-M-O14	90.62(3)	90.32(2)	91.54(3)
	O11-M-O12	96.50(3)	94.61(2)	93.54(2)
	O11-M-O14	89.18(3)	89.33(2)	89.86(2)
	O12-M-O14	173.65(3)	175.30(2)	175.78(2)
	S1-O11	145.51(7)	145.53(5)	145.80(6)
	S1-O12	146.27(7)	146.42(5)	146.25(6)
	S1-O13	144.58(7)	145.05(5)	144.87(6)
	S1-C1	178.01(9)	177.83(6)	177.99(7)
	S2-O14	146.59(7)	146.69(5)	146.72(6)
	S2-O15	144.98(8)	145.10(6)	145.01(7)
	S2-O16	144.62(8)	144.73(6)	144.83(7)
	S2-C4	177.37(10)	177.32(7)	177.60(8)
O11-S1-O12	111.99(4)	112.30(3)	112.53(4)	
	112.41(4)	112.33(3)	112.11(4)	
	112.92(4)	112.83(3)	112.74(4)	
	108.03(4)	108.45(3)	108.50(3)	
	105.24(4)	105.00(3)	104.88(3)	
	105.66(4)	105.31(3)	105.48(4)	
O14-S2-O15	111.56(5)	111.62(4)	111.53(4)	
	112.21(5)	112.01(4)	111.89(4)	
	114.77(5)	114.68(4)	114.78(4)	
	104.95(4)	105.45(3)	105.70(4)	
	106.30(5)	106.17(3)	106.20(4)	
	106.21(5)	106.14(3)	105.98(4)	

into a glass ampoule, which was torch-sealed under vacuum. The ampoule was placed in a resistance furnace and heated up to 120 °C for 6 h. After 36 h, the furnace was slowly cooled to room temperature within 120 h. The product was obtained as transparent pink single crystals, which were separated from the supernatant by decantation.

IR(ATR): 2972 (w), 2934 (w), 2885 (w), 1642 (s), 1515 (m), 1481 (w), 1462 (w), 1448 (m), 1427 (m), 1410 (m), 1393 (m), 1306 (m), 1260 (w), 1214 (s), 1174 (s), 1106 (m), 1036 (s), 1002 (s), 929 (w), 835 (m), 730 (m), 659 (s), 618 (m), 579 (m), 549 (m), 542 (m) cm^{-1} .

X-ray crystallography

The data for the X-ray single crystal structure determinations were collected on a Bruker Apex II CCD diffractometer. For that purpose, the single crystals were selected under protecting oil

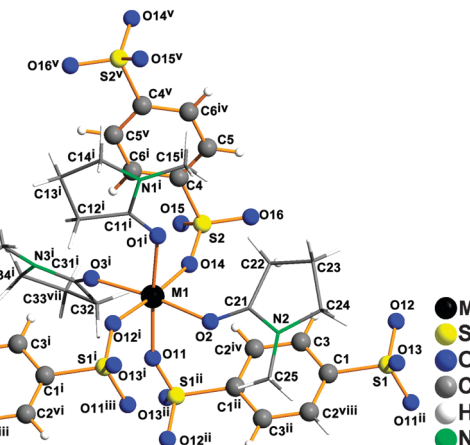


Fig. 1 Coordination of the M^{2+} cations in the crystal structures of $M(BDS)-(NMP)_3$ ($M = Mn, Fe, Co$). Note that both disulfonate anions bear inversion symmetry. Within the $[MO_6]$ octahedron, the bond $M-O1$ is the longest in all of the three compounds, according to the *trans* effect caused by the opposite sulfonate anion. The NMP molecules are drawn in a wire model for clarity. Symmetry codes: (i) = $1 + x, y, z$; (ii) = $1 - x, 1 - y, -z$; (iii) = $2 - x, 1 - y, -z$; (iv) = $1 - x, 1 - y, 1 - z$; (v) = $2 - x, 1, y, 1 - z$; (vi) = $1 + x, y, -1 + z$; (vii) = $1 + x, 1 + y, z$; (viii) = $x, y, -1 + z$.

and transferred directly into the cool nitrogen stream of the diffractometer. Details of the data collections are summarized in Tables 1 and 2. The structures were solved using Direct Methods (SHELXS-97) and refined by full-matrix least-squares method (SHELXL-97). All non-hydrogen atoms were refined with anisotropic displacement parameters in the course of the structure refinement. The positions of the hydrogen atoms were located from the Fourier difference maps at the final stage of the refinements. They were refined using a riding model with the relative isotropic parameters of the heavy atoms to which they are attached.

X-ray powder diffraction investigations were performed with the help of a powder diffractometer STADI P (STOE) with $\text{Cu-K}\alpha 1$ radiation using a flat sample holder or thin-walled glass capillaries.

Results and discussion

Crystal structures

The three disulfonates $M(BDS)(NMP)_3$ ($M = Mn, Fe, Co$) are isotopic with each other and crystallize with triclinic symmetry (space group $P\bar{1}$). In accordance with the decreasing ionic radii, the unit cell volume shrinks in the order $Mn > Fe > Co$ (Table 1). The crystal structures show one crystallographically independent M^{2+} ion, which is in octahedral coordination of six oxygen atoms. The oxygen atoms belong to three benzenedisulfonate anions and three NMP molecules (Fig. 1). NMP was used as the solvent because it is aprotic and can solvate the acid and metal salts well. The distances $M-O$ between the metal atom and the oxygen atoms of the sulfonate groups range from 216.45(7) to 218.83(7) pm for $M = Mn$, 213.07(5) to 214.65(5) pm for $M = Fe$, and 209.44(6) to 210.23(6) pm for $M = Co$. The distances $M-O_{\text{solv}}$ between the metal atoms and the oxygen



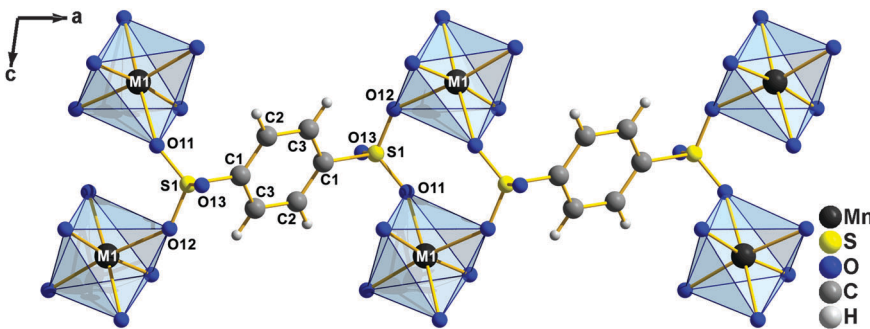


Fig. 2 In the crystal structures of $M(BDS)(NMP)_3$ ($M = Mn, Fe, Co$), one type of benzene disulfonate anion, BDS1, acts as a tetradentate bridging ligand connecting four M^{2+} ions with each other into infinite chains running along the crystallographic [100] direction.

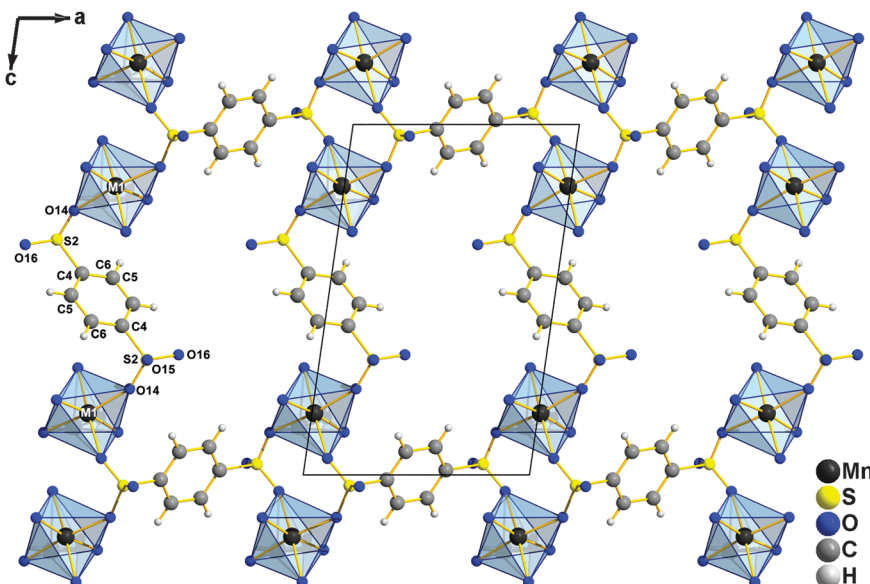


Fig. 3 The second type of benzene disulfonate anion, BDS2, in the crystal structures of $M(BDS)(NMP)_3$ ($M = Mn, Fe, Co$) acts as bidentate ligand and connects the chains shown in Fig. 2 yielding layers according to $\infty^2[Mn(BDS1)_{2/4}(BDS2)_{1/2}(NMP)_{3/1}]$, which expand in the (010).

atoms of the solvent molecules are significantly enlarged for oxygen atoms that are situated in *trans* position to a sulfonate ligand. They show values of 220.78(7) pm ($M = Mn$), 216.49(5) pm ($M = Fe$), and 212.75(6) pm ($M = Co$), which are about 5–10 pm longer than the distances observed for the remaining two NMP molecules (Table 2).

The three M^{2+} coordinated benzene disulfonate anions belong to two crystallographically different species, BDS1 and BDS2. Both anions bear inversion symmetry because the centroids of the anion benzene rings are situated onto the Wyckoff positions 1e ($1/2, 1/2, 0$) and 1g ($0, 1/2, 1/2$) of the triclinic unit cell. Both disulfonate anions behave differently with respect to their cation linkage. The anion BDS1 connects four M^{2+} ions with each other (Fig. 2). This is achieved by a bidentate bridging coordination mode of the two symmetry equivalent $[\text{SO}_3]$ groups of the anions and the linkage leads to chains running along the [100] direction. These chains are further connected by the second type of anions, BDS2, which show each of the $[\text{SO}_3]$ groups in monodentate coordination to the M^{2+} ions.

In this way, layers are formed according to the Niggli formula $\infty^2[Mn(BDS1)_{2/4}(BDS2)_{1/2}(NMP)_{3/1}]$ that expand in the (010) plane (Fig. 3). The layers $\infty^2[Mn(BDS1)_{2/4}(BDS2)_{1/2}(NMP)_{3/1}]$ are stacked along the [010] direction (Fig. 4). Only weak interactions between the layers can be assumed because the NMP molecules are not capable of forming hydrogen bonds with non-coordinating oxygen atoms of the anions. This also explains the high cleavability of the crystals. It is interesting to compare the structural features of the compounds $M(BDS)(NMP)_3$ ($M = Mn, Fe, Co$) with the recently reported manganese disulfonate $Mn(BDS)(NMP)_2$.¹¹ The latter also shows a layer structure but due to the lower solvent content, all the disulfonate anions act as bidentate bridging ligands according to $\infty^2[Mn(BDS)_{4/4}(NMP)_{2/1}]$. Following this line, the further reduction of solvent molecules should lead to three-dimensional networks according to $\infty^3[Mn(BDS1)_{3/6}(BDS2)_{2/4}(NMP)_{1/1}]$ for $Mn(BDS)(NMP)$ and $\infty^3[Mn(BDS)_{6/6}]$ for the solvent-free compound. In turn, a higher content of solvent molecules could lead to chain type structures for the composition $Mn(BDS)(NMP)_4$ and to monomeric compounds



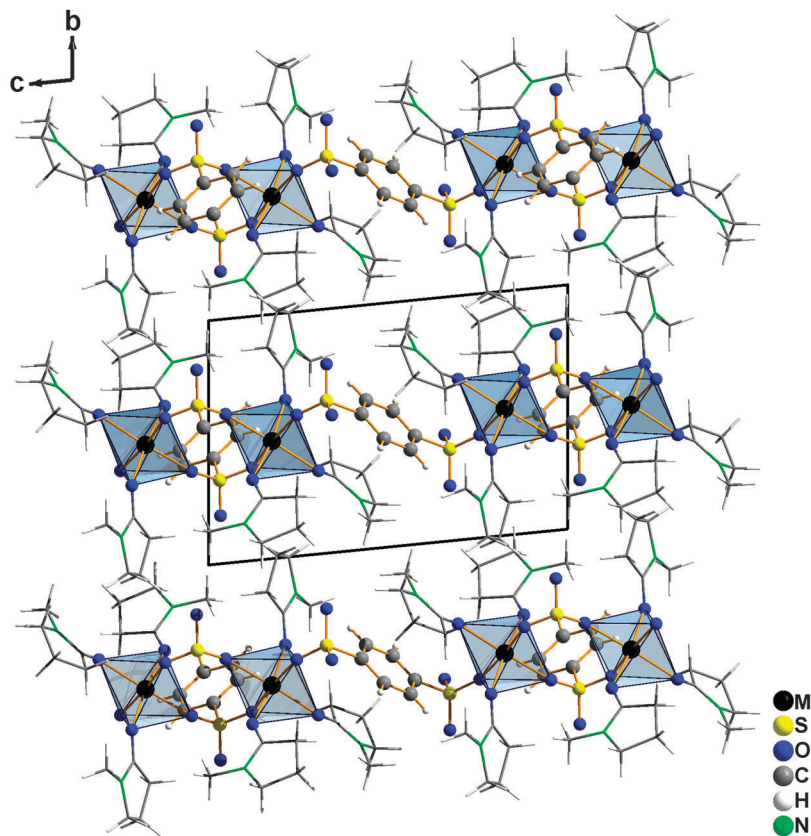


Fig. 4 Crystal structure of the disulfonates $M(BDS)(NMP)_3$ ($M = Mn, Fe, Co$) viewed along [100]. The layers $\infty^2[Mn(BDS1)_{2/4}(BDS2)_{1/2}(NMP)_{3/1}]$ are stacked along the [010] direction. The NMP molecules are drawn in a wire model for clarity.

for $Mn(BDS)(NMP)_5$ and $Mn(BDS)(NMP)_6$. Even if this has not been proved up to now, there are comparable compounds that foster this assumption: the zinc compound $Zn(BDS_4)(DMF)_4$ bearing the tetrafluoro derivative of BDS and dimethylformamide as solvent exhibits exactly the expected chain structure. Moreover, we could characterize $Fe(BDS)(H_2O)_3(NMP)_2$ as a hydrolyzation product of $Fe(BDS)(NMP)_3$, which can be seen as an example for $M(BDS)(L)_5$ type compounds when L is a neutral ligand. This compound indeed shows a molecular structure with monodentate sulfonate anions.¹⁴ Finally, the copper sulfonate $[Cu(H_2O)_6](BDS)$ is a nice example for a solvent-rich disulfonate showing the

exclusive solvent coordination of the cation.³ Solvent poor species are especially highly esteemed targets of our ongoing research.

Thermal analysis

All the disulfonates have been investigated by means of thermal analyses. The measurements have been performed under flowing oxygen. This makes sure that there is no carbon left in the decomposition residues, which is often observed as amorphous decomposition product causing high backgrounds in the diffraction patterns. For $Mn(BDS)(NMP)_3$, the desolvation is a two-step process between 150 and 215 °C (Fig. 5). According to the

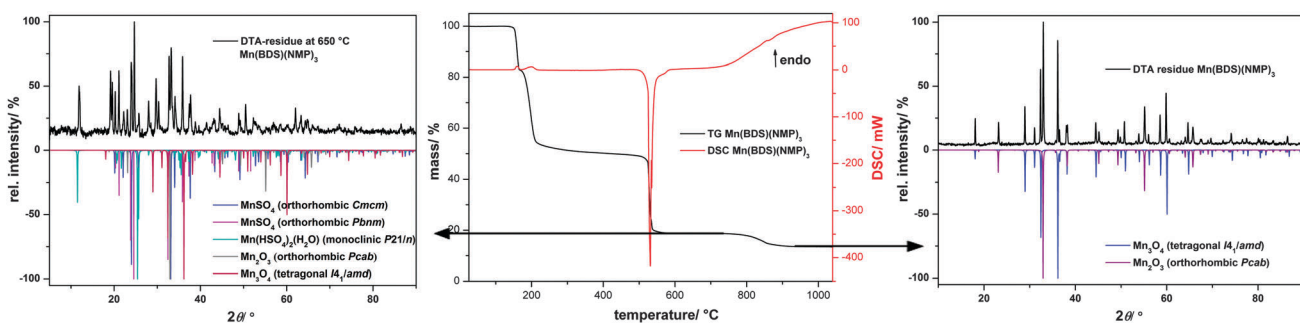


Fig. 5 Thermal decomposition of $Mn(BDS)(NMP)_3$. The DSC/TG diagram (middle) shows that the compound is desolvated upon heating. The solvent-free compound decomposes, yielding a mixture of manganese sulfates and oxides (X-ray powder pattern shown left), and finally a mixture of Mn_2O_3 and Mn_3O_4 (X-ray powder pattern shown right). The DSC/TG measurements were performed under oxygen flow.

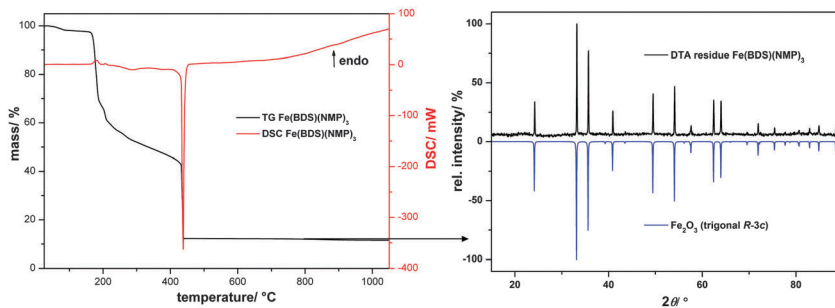


Fig. 6 Thermal decomposition of $\text{Fe}(\text{BDS})(\text{NMP})_3$. The DSC/TG diagram (left) shows that after desolvation there is no significant plateau. After decomposition of the desolvated sulfonates, the oxide Fe_2O_3 is obtained (X-ray powder pattern shown right). The DSC/TG measurements were performed under oxygen flow.

observed mass loss of 49% (calcd 51% for three molecules of NMP), the desolvation is completed above that temperature. Unfortunately, the solvent-free disulfonates are X-ray amorphous, and therefore no structural information can be gained by diffraction methods. The solvent-free disulfonate $[\text{Mn}(\text{BDS})]$ is remarkably stable and decomposes only above a temperature of $500\text{ }^\circ\text{C}$ ($T_{\text{max}} = 530\text{ }^\circ\text{C}$). The decomposition is exothermic and occurs in the temperature range from $520\text{ }^\circ\text{C}$ to $545\text{ }^\circ\text{C}$. According to X-ray powder investigations, the decomposition product at this stage is a mixture of MnSO_4 , Mn_2O_3 and Mn_3O_4 (Fig. 5). The observed reflections also suggest the presence of some amounts of $\text{Mn}(\text{HSO}_4)_2(\text{H}_2\text{O})$, which is probably caused by the reaction of the sample with moisture during the X-ray measurement. Finally, between $837\text{ }^\circ\text{C}$ and $862\text{ }^\circ\text{C}$, the oxides Mn_3O_4 and Mn_2O_3 are obtained in a ratio of 16:9 according the observed mass loss of 13%. The loss of solvent molecules is also the first decomposition step for $\text{Fe}(\text{BDS})(\text{NMP})_3$. Moreover, the desolvation is a two-step

process, and it is completed at about $330\text{ }^\circ\text{C}$ (Fig. 6). The correlated mass loss is 50% at that temperature, in line with the calculated value (51%). However, compared to the manganese compound, the plateau in the TG curve is not very significant and a creeping mass loss is observed. The decomposition of the intermediate $[\text{Fe}(\text{BDS})]$ occurs in the temperature range between 432 and $444\text{ }^\circ\text{C}$, *i.e.*, at significantly lower temperature than observed for $[\text{Mn}(\text{BDS})]$, and no sulfate intermediate could be detected. Instead, corundum type Fe_2O_3 is directly formed, as indicated by X-ray powder diffraction (mass loss: 12%, calcd 14%) (Fig. 6). For $\text{Co}(\text{BDS})(\text{NMP})_3$, the two-step desolvation is completed at $180\text{ }^\circ\text{C}$ (Fig. 7), and the desolvated compound starts to decompose at $520\text{ }^\circ\text{C}$. This decomposition leads to an intermediate consisting of CoSO_4 and Co_3O_4 . Small amounts of $\text{Co}(\text{SO}_4)(\text{H}_2\text{O})_2$ are due to reaction of the sample with moisture during the X-ray measurement. At a temperature above $813\text{ }^\circ\text{C}$ ($T_{\text{max}} = 835\text{ }^\circ\text{C}$), Co_3O_4 is the only decomposition product. Co_3O_4 melts

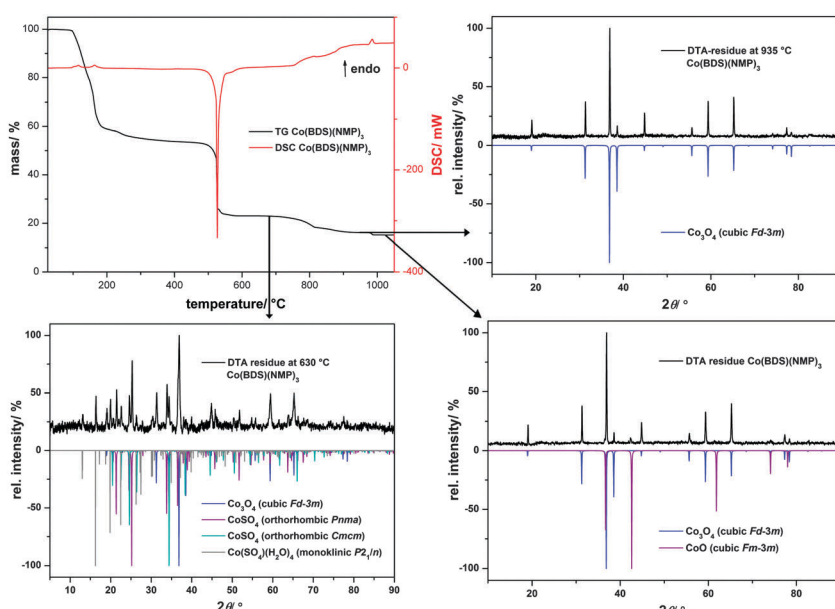


Fig. 7 Thermal decomposition of $\text{Co}(\text{BDS})(\text{NMP})_3$. The DSC/TG diagram (upper part, left) shows that the compound decomposes after desolvation in three steps. Firstly, Co_3O_4 is formed along with some amounts of CoSO_4 (lower part, left). In a further step, the latter is transformed to Co_3O_4 (upper part, right), which finally starts to decompose to CoO (lower part, right).

Table 3 Data for the thermal decomposition of the disulfonates M(BDS)(NMP)₃

Stage	T _{onset} /°C	T _{end} /°C	T _{max} /°C	Mass loss obsd/%	Mass loss calcd/%	Elimination/decomposition
Mn(BDS)(NMP)₃						
I	150	215	160; 200	49	51	Loss of three equiv. of NMP
II	520	545	530	32	—	Decomposition to MnSO ₄ , Mn(HSO ₄) ₂ (H ₂ O) ^a , Mn ₂ O ₃ and Mn ₃ O ₄
III	837	862	855	6	—	Decomposition to 16Mn ₃ O ₄ and 9Mn ₂ O ₃ (calcd 13%)
Σ				87	—	
Fe(BDS)(NMP)₃						
I	50	330	180; 205; 285	50	50	Loss of three equiv. of NMP
II	432	444	438	38	36	Decomposition to Fe ₂ O ₃ (calcd 14%)
Σ				88	86	
Co(BDS)(NMP)₃						
I	96	180	115; 163	46	50	Loss of three equiv. of NMP
II	520	592	527	31	—	Decomposition to CoSO ₄ , Co(SO ₄) ₂ (H ₂ O) ^a and Co ₃ O ₄
III	754	835	813	7	—	Decomposition of Co ₃ O ₄ (and small amount of CoO) ^b (calcd 14%) ^b
IV	974	992	985	1	—	Melting and evaporation of Co ₃ O ₄
Σ				85	—	

^a The hydrates are probably caused by reaction of the sample with moisture during the measurement. ^b In the calculation the amount of CoO is not included.

according to the literature at about 900 °C.¹⁵ Herein, we observed the melting point of Co₃O₄ at 985 °C, followed by slow decomposition to CoO (Fig. 7). The thermoanalytical data are summarized in Table 3.

Conclusion

In the present study, we have shown that 1,4-benzenedisulfonic acid (H₂BDS), a sulfo analogue of terephthalic acid, is a suitable candidate for the preparation of two-dimensional coordination polymers of manganese, iron, and cobalt. The disulfonates crystallize as solvates M(BDS)(NMP)₃ (M = Mn, Fe and Co) when *N*-methyl-pyrrolidone is used as the solvent. The BDS²⁻ ligands act either as tetradentate or bidentate bridging ligands. The most important characteristic of the compounds is that the solvent molecules can be easily removed by heating. The desolvated compounds are remarkably stable for the metals manganese and cobalt even up to 530 °C. This is clearly above the values that have been reported for comparable terephthalate compounds. Our future work aims at the comprehensive exploration of the structural chemistry of polysulfonates and their properties.

Acknowledgements

Financial support of the *Deutsche Forschungsgemeinschaft* is gratefully acknowledged. We are thankful to Dipl.-Chem. Wolfgang Saak and Dr Marc Schmidtmann for the collection of the X-ray data, and to Florian Behler for IR-spectroscopic measurements.

References

- Recent reviews: (a) S. Ma and H.-C. Zhou, *Chem. Commun.*, 2010, **46**, 44; (b) Z. Wang and S. M. Cohen, *Chem. Soc. Rev.*, 2009, **38**, 1315; (c) D. Farrusseng, S. Aguado and C. Pinel, *Angew. Chem.*, 2009, **121**, 7638 (*Angew. Chem., Int. Ed.*, 2009, **48**, 7502); (d) R. A. Fischer and C. Wöll, *Angew. Chem.*, 2008,

120, 8285 (*Angew. Chem., Int. Ed.*, 2008, **47**, 8164); (e) S. Bauer and N. Stock, *Chem. Unserer Zeit*, 2008, **42**, 12; (f) U. Müller, M. Schubert, F. Teich, H. Pütter, K. Schierle-Arndt and J. Pastre, *J. Mater. Chem.*, 2006, **16**, 626; (g) S. Kaskel, *Nachr. Chem.*, 2005, **53**, 394; (h) J. L. C. Rowsell and O. M. Yaghi, *Angew. Chem.*, 2005, **117**, 4748 (*Angew. Chem., Int. Ed.*, 2005, **44**, 4670).

- G. P. Panasyuk, L. A. Azarova, G. P. Budova and A. P. Savost'yanov, *Inorg. Mater.*, 2007, **43**, 951.
- T. W. T. Muesmann, C. Zitzer, A. Mietrach, T. Klüner, J. Christoffers and M. S. Wickleder, *Dalton Trans.*, 2011, **40**, 3128.
- (a) B. D. Chandler, G. D. Enright, K. A. Udachin, S. Pawsey, J. A. Ripmeester, D. T. Cramb and G. K. H. Shimizu, *Nat. Mater.*, 2008, **7**, 229; (b) Review: G. K. H. Shimizu, R. Vaidhyanathan and J. M. Taylor, *Chem. Soc. Rev.*, 2009, **38**, 1430.
- (a) T. Z. Forbes and S. C. Sevov, *Inorg. Chem.*, 2009, **48**, 6873; (b) J. S. Haynes, S. J. Rettig, J. R. Sams, R. C. Thompson and J. Trotter, *Can. J. Chem.*, 1986, **64**, 429.
- (a) R.-G. Xiong, J. Zhang, Z.-F. Chen, X.-Z. You, C.-M. Che and H.-K. Fun, *J. Chem. Soc., Dalton Trans.*, 2001, 780; (b) W. Wan, Z.-B. Zhu, L.-H. Huo, Z.-P. Deng, H. Zhao and S. Gao, *CrystEngComm*, 2012, **14**, 5274; (c) Q.-Y. Liu, Z.-J. Xiahou, Y.-L. Wang, L.-Q. Li, L.-L. Chen and Y. Fu, *CrystEngComm*, 2013, **15**, 4930; (d) Y.-H. Zhang, X. Li, S. Song, H.-Y. Yang, D. Ma and Y.-H. Liu, *CrystEngComm*, 2014, **16**, 8390.
- F. Gándara, C. Fortes-Revilla, N. Snejko, E. Gutiérrez-Puebla, M. Iglesias and M. A. Monge, *Inorg. Chem.*, 2006, **45**, 9680.
- (a) T. W. T. Muesmann, M. S. Wickleder and J. Christoffers, *Synthesis*, 2011, 2775; (b) T. W. T. Muesmann, M. S. Wickleder, C. Zitzer and J. Christoffers, *Synlett*, 2013, 959.
- (a) T. W. T. Muesmann, A. Mietrach, J. Christoffers and M. S. Wickleder, *Z. Anorg. Allg. Chem.*, 2010, **636**, 1307; (b) A. Mietrach, T. W. T. Muesmann, C. Zilinski, J. Christoffers and M. S. Wickleder, *Z. Anorg. Allg. Chem.*, 2011, **637**, 195;



(c) T. W. T. Muesmann, C. Zitzer, M. S. Wickleder and J. Christoffers, *Inorg. Chim. Acta*, 2011, **369**, 45; (d) T. W. T. Muesmann, J. Ohlert, M. S. Wickleder and J. Christoffers, *Eur. J. Org. Chem.*, 2011, 1695.

10 A. Mietrach, T. W. T. Muesmann, J. Christoffers and M. S. Wickleder, *Eur. J. Inorg. Chem.*, 2009, 5328.

11 C. Zitzer, T. W. T. Muesmann, J. Christoffers, C. Schwickert, R. Pöttgen and M. S. Wickleder, *CrystEngComm*, 2014, **16**, 11064.

12 (a) A. Carton, A. Mesbah, L. Perrin and M. François, *Acta Crystallogr., Sect. E: Struct. Rep. Online*, 2007, **63**, m948; (b) S. C. Manna, E. Zangrando, J. Ribas and N. R. Chaudjuri, *Dalton Trans.*, 2007, 1383; (c) H. X. Zhang, B.-S. Kang, A.-W. Xu, Z.-N. Chen, Z.-Y. Zhou, A. S. C. Chan, K.-B. Yu and C. Ren, *J. Chem. Soc., Dalton Trans.*, 2001, 2559; (d) K.-Y. Choi, K.-M. Chun, K.-C. Lee and J. Kim, *Polyhedron*, 2002, **21**, 1913; (e) B.-L. Chen, K.-F. Mok, S.-C. Ng and M. G. B. Drew, *New J. Chem.*, 1999, **23**, 877; (f) C. S. Hong and Y. Do, *Inorg. Chem.*, 1997, **36**, 5684; (g) H.-K. Fun, S. S. S. Raj, R.-G. Xiong, J.-L. Zuo, Z. Yu and X.-Z. You, *J. Chem. Soc., Dalton Trans.*, 1999, 1915; (h) U. Mueller, M. Schubert, F. Teich, H. Puetter, K. Schierle-Arndt and J. Pastré, *J. Mater. Chem.*, 2006, **16**, 626; (i) H. Li, M. Eddaoudi, M. O'Keeffe and O. M. Yaghi, *Nature*, 1999, **402**, 276; (j) M. Eddaoudi, H. Li and O. M. Yaghi, *J. Am. Chem. Soc.*, 2000, **122**, 1391.

13 Star^e V 9.3, Mettler-Toledo GmbH, Schwerzenbach, Switzerland, 2009.

14 C. Zitzer, T. W. T. Muesmann, J. Christoffers and M. S. Wickleder, *Z. Kristallogr. NCS*, 2014, **229**, 103.

15 A. F. Holleman, E. Wiberg, N. Wiberg, 102. Auflage, Lehrbuch der anorganischen Chemie, de Gruyter, Berlin, New York, 2007.

